International Journal of Metallurgical &
Materials Science and Engineering (IJMMSE)
ISSN(P): 2278-2516; ISSN(E): 2278-2524
Vol. 5, Issue 2, Apr 2015, 17-28

EFFECT OF CHROMIUM AND SILICON ADDITIONS ON THE MICROSTRUCTURE AND MECHANICAL PROPERTIES OF COMPLEX ALUMINUM BRONZE

K. S. ABDEL-WAHAB[1], A. A. HUSSEIN[2], E. M. EL BANNA[3] & M. A. WALY[4]

[1,4]Central Metallurgical R&D Institute (CMRDI), Helwan, Egypt

[2,3]Department of Metallurgy, Faculty of Engineering, Cairo University, Egypt

ABSTRACT

Cast nickel-aluminum bronze (NAB) is the best material of choice for propellers in both surface ships and submarines. New designs require a material with improved strength, hardness and high wear resistance. The mechanical properties of the NAB alloy are largely dependent on the kappa (κ) phase characteristics (i.e. size, morphology and distribution).

In the present study, the refinement and modification performance of Cr and Si on the kappa phases in the nickel aluminum bronze alloy were investigated. The microstructure of as cast alloys was examined by optical microscope and scanning electron microscope (SEM). Different phases were detected. The experimental results showed that the Cr and Si modified the kappa phases (κ) and crystallized in a form of complex silicides rich in iron, chromium and silicon. A refinement of the grain size of α matrix from 56±6 µm to 32±2 µm was successfully accomplished by such alloy additions. The complex silicides are precipitated in β-phase and cause a refinement of the microstructure by providing sites for the nucleation of the α-phase, to some extent, by impeding the growth of the α-phase. The mechanical properties were determined by tensile, hardness and wear tests. The micro hardness of α and κ phases was also measured. Significant improvements in the mechanical properties have been obtained by a combination of grain refinement and modification of the NAB alloy.

KEYWORDS: Aluminum Bronze, Grain Refinement, Kappa Phase, Microstructure and Mechanical Properties

INTRODUCTION

Nickel-aluminum bronze (NAB) refers to copper-based alloys with aluminum, nickel and iron as primary additions, with smaller amounts of manganese added as well. NAB alloys are used extensively for marine applications such as propellers, pumps, gears and valve components. NAB exhibits excellent corrosion resistance as well as good strength making it a material of choice for marine applications for naval surface and subsurface platforms. In addition to its overall strength and corrosion resistance, NAB has other attributes. These include: i) non-sparking behavior, ii) good wear ability and low friction coefficients, iii) good fracture toughness at both elevated and lower temperatures, iv) high damping capacity to reduce noise transmissions, and v) exceptional resistance to fatigue which is a leading cause to material deterioration and failure in marine equipment [1-5].

Under normal casting conditions, the alloy has a microstructure consisting of an fcc Cu-rich solid solution or α-phase, several intermetallic phases collectively referred to as κ-phase, and some "retained β-phase"[6-8]. The κ_i precipitates have a dendritic morphology and are cored; the composition ranges from iron-rich solid solution to Fe_3AI. The κ_{ii} and κ_{iv}

precipitates have, respectively, a dendritic and an equiaxed/dendritic morphology, and are based on Fe_3A1, while κ_{iii} is a eutectoidal decomposition product of lamellar or globular morphology based on NiA1.

The κ-phases found in the present study are relatively hard and brittle. These precipitates seriously separate α matrix and thus cause alloy embrittlement [5,7-11].

Further alloying additions to the (NAB) alloy have been attempted aiming at further improving the mechanical properties and grain refinement. Results of current researches have shown that the mechanism of grain refinement in copper-base alloys is not well understood. This lack of understanding extends to the interaction between the grain refiner and the other elements present in copper alloys such as Sn, Al, Bi, Se and Pb. The evaluation of nuclei formation, which causes the grain refinement in copper alloys, is also necessary. The results so far published is still lacking for the successful additions to further enhancing the mechanical properties particularly wear resistance. This work is thus planed to modify the standard (NAB) alloy with additions of chromium and silicon. Besides fulfilling the requirements of grain refinement and improved wear resistance, a detailed study of phase formation is planned.

EXPERIMENTAL PROCEDURE

Commercial grade NAB alloy was used as the base alloy for this investigation. This commercial grade prepared by melting of electrolytic copper, commercial pure aluminum, electrolytic nickel and low alloy steel scrape as a source of iron. The chemical compositions of the investigated alloys are given in Table 1. Required amounts of Cr and Si were added in the form of low carbon ferro-chrome master alloy and pure silicon respectively.

Investigated material were prepared in four categories, in order to determine the optimum amount and effective element in modification as follows:

- Reference based alloy (prepared commercial NAB).
- With chromium addition.
- With Silicon addition.
- Both silicon and chromium addition.

Melting process was carried out in a medium frequency induction furnace with silicon carbide crucible. The charging materials were started firstly with electrolytic copper and calculated amount of nickel and iron. Nickel was added as electrolytic nickel, where iron was added as low alloy steel scrape and the proper amount of pure aluminum was added to melt. After completely melting of the charging material, the melt was held at temperature of 1200 $^{\circ}$C for five minutes in order to achieve completely mixing of all charging elements. During melting, a layer of charcoal with a thickness of 20–30mm were used in order to protect liquid metal from oxidation, to decrease the amount of oxygen absorbed during melting and increase the heat rate by its ignition. The proper amounts of silicon or chromium were added according to weight percent described in table 3.1. Finally to accentuate the chemical composition of each alloy, a chemical analysis sample was extracted from melt and analyzed by the help of a spark emission spectrometry. The pouring temperature was adjusted by measuring twice using a thermocouple type S one just before handling the molten metal from the furnace and the other was just before pouring. Finally pouring process was carried out in a sand mold at a temperature of 1200±10 $^{\circ}$C after deslagging by graphite rod. The dimensions of produced cast piece is described in Figure 3.2, which also showed the extraction of the tensile test specimen.

The as-cast specimens were prepared by standard metallographic techniques which consist of polishing and etching in an etchant composed of 1 g $FeCl_3$, 20ml HCl, and 100 ml distilled water. After etching, the specimens were observed under optical and scanning electron microscope.

Table 1: Chemical Composition (wt %) of Cast Specimens

Element / Alloy	Cu	Al	Fe	Ni	Mn	Si	Cr
NAB alloy	81.68	9.39	4.14	4.00	1.06	0.001	0.005
NAB+ 0.4% Cr	79.39	10.25	4.71	5.05	1.25	0.007	0.400
NAB + 0.8% Cr	81.14	9.66	4.23	4.05	1.35	0.010	0.800
NAB + 0.5% Si	80.43	9.50	4.60	5.16	1.07	0.500	0.009
NAB +0.2% Cr+ 0.5%Si	80.54	9.40	4.30	3.73	1.50	0.500	0.230

Tensile specimens according to ASTM E8 were machined using Electric Discharge Machning (EDM). The tensile tests were carried out at room temperature at a strain rate of 0.5 mm/sec.

The average grain size of each sample was measured. Linear intercept method according to ASTM standard E11288 was used to evaluate the grain size. The average bulk Vickers hardness (HV30) of the specimens was measured. The applied load was 30 kg, loading time was 60 seconds. An average of 10 observations has been considered in this study. Microhardness determinations were carried out using a HMV SHIMADZU microhardness tester with a diamond pyramid indentor, a 100 gram load and test time of 15 seconds. An average of 3 observations has been considered in this study. A pen on disk wear testing process was used to measure the weight loss of the specimens with 265 rpm speed, 0.5 bar load and 20 min applied time.

RESULT AND DISCUSSIONS

Optical Microstructure

Microstructure of the present cast alloy with and without Cr and Si additions are presented in Figure 1. Atypical microstructure of the unmodified NAB alloy is shown in Figure 1a, which demonstrates a substantial microstructural difference in the size, morphology and distribution of **κ** phases, This alloy consisting mainly of coarse-grained **α** as matrix (light color), **β'** or retained **β** (darkest regions), and several intermetallic phases such as $\boldsymbol{\kappa_{ii}}$, $\boldsymbol{\kappa_{iii}}$ and $\boldsymbol{\kappa_{iv}}$ which is confirmed by Mokhtari et al [6] Where, κ_{ii} appear as dendrite structures precipitate in α phase. Also, κ_{ii} is an iron-rich phase (based on Fe_3Al). Moreover, κ_{iii} is a nickel-rich phase (NiAl) and appears as a lamellar eutectoid structure that coexists with α phase. Finally, κ_{iv} is an iron-rich phase, mostly appears as fine round particles embedded in matrix [5- 11]. The average grain size for this cast structure as determined is **56±6 μm** and the non-equilibrium cooling conditions naturally resulted in dendrite structure and also segregation to grain and sub grain boundaries.

Addition of 0.4 wt% chromium resulted in apparently refinement of α grain size as demonstrated in Figure 1b. The average grain size for this cast structure is 44±4 **μm**. The two alloys (NAB and NAB + 0.4% Cr) have some common characteristics, for example, they both have **α** phase, retained **β** and **κ** phases. As shown in the micrograph of Figure 1b, in the chromium modified alloy, the microstructure consists of colonies, predominantly of κ phase that precipitated at grain boundaries of α matrix. These precipitates inhibited the growth of alpha phase and thus reduce their size. The chromium additions also influence the relative content of the phase, their sizes of phase and their shape and distribution. The chromium additions cause additional formation of very fine and spherical Fe-rich $\boldsymbol{\kappa_{iv}}$ phase within α grain.

It can be seen that $\kappa_{ii\ (Cr)}$ phase became fine and well defined after addition of chromium, but the morphology was still dendritic. The results of EDS elemental mapping for $\kappa_{ii\ (Cr)}$ precipitates showed it contained high concentration of iron and chromium as shown in Figure 2. Based on the fact that chromium dissolves partially in copper but it solubility in iron is high [12] so, it dissolves in the larger stage in κ_{ii} and κ_{iv} precipitates exclusively (that contains high concentration of Fe) than in κ_{iii} precipitates (contains high concentration of Ni). This makes these precipitates crystallized as large complex compounds $\kappa_{ii\ (Cr)}$ and $\kappa_{iv\ (Cr)}$, composed of Fe and Cr distributed at the grain boundaries of α matrix [12-18].

Raising the chromium content to 0.8 wt% resulted in increased grain size to **64±6** μm**.** As can be seen in Figure 1c the microstructure of the alloy comprises of large alpha grains. Inside these grains, there are more amounts of the complex compounds **($\kappa_{ii\ (Cr)}$)** phase with large irregular shape as a result of increasing chromium content as shown in Figure 1d. These complex compounds are precipitate in the matrix which led to decreases grain locking effects and increases the alpha grain size. Also, lamellar eutectoid (**α** + κ_{iii}) areas occur at grain boundaries of alpha matrix. A ″new″ phase **($\acute{\kappa}_{iii}$)** having a butterfly shape appears inside α grain as can be showed in both optical and SEM micrographs (Figure 1c and Figure 3). In addition, there are fine $\kappa_{iv\ (Cr)}$ precipitates inside the **α**-grains**.** The EDS micro analysis of the new $\acute{\kappa}_{iii}$ phase (Figure 4) reveals their content of 48 wt% Cu, 35 wt% Ni, 9 wt% Al, 5 wt% Fe and little amounts of Cr and Mn. This micro analysis apparently similar to the micro analysis of κ_{iii} precipitates that present in as cast NAB alloy without addition of modifier elements [7-11]. Most of these compounds are precipitated in separate groups within α-grains thus lead to a decrease in the grain locking effect and an increased **α** grain size.

Additions of 0.5% Si to the NAB alloy are reported to lead much finer grain sizes compared to those unmodified and chromium treated alloys as shown in Figure 1e, The structure is still a mixture of **α** matrix and kappa phases and the grain size is refined from **56±6 μm** for the unmodified alloy to **32±2 μm**.

This is generally believed to be a result of the formation of complex silicides of the iron $\kappa_{ii\ (Si)}$ during the early stages of solidification which inhibit the growth of alpha grain. There are much finer and spherical $\kappa_{iv(Si)}$ precipitates in **α** matrix compared to unmodified alloy. Also, there is increase in amount of $\kappa_{ii(Si)}$ precipitates that are smaller and well defined compared to the previous alloys. The grain boundaries appear with fewer precipitates and all phases disperse more homogeneously in the **α**-matrix than in the above alloys, which expectedly may lead to an enhancement of the mechanical properties of this alloy.

Earlier research [12] has shown that silicon is pushed aside before the front of the crystallization of phase β from all elements creators of solid solutions with the copper the most intensely and created intermetallic phases rich in iron and silicon can have the structure of the complex silicides of the iron κ_{FeSi}. These precipitates are formed before the nucleation of α phase. Since the α-phase nucleates both at the β-phase grain boundaries and at the iron-rich particles **(κ_{FeSi})** inside the β-grains, the number of nucleation sites for α is large and the consequent mean phase size is small. Also, the growth of α-phase during further cooling appears to be hampered by the iron-rich particles, and this imposes an additional restriction on the eventual size of α-phase precipitates which may cause some refinement of the as-cast microstructure.

Combined additions of 0.5 wt% silicon and 0.2wt% chromium to the NAB alloy are reported to the same grain size of the NAB alloy treated with 0.5 wt% Si. The grain size was **34±2μm**. The microstructure of alloy is generally similar to the NAB alloy treated with 0.5% Si. The $\kappa_{ii(CrSi)}$ precipitates turn to become smaller and globular in shape. Additionally, large amounts of fine $\kappa_{iv\ (CrSi)}$ precipitates appear dispersed in the α-matrix (Figure 1f). This dispersion again leads to grain refinement.

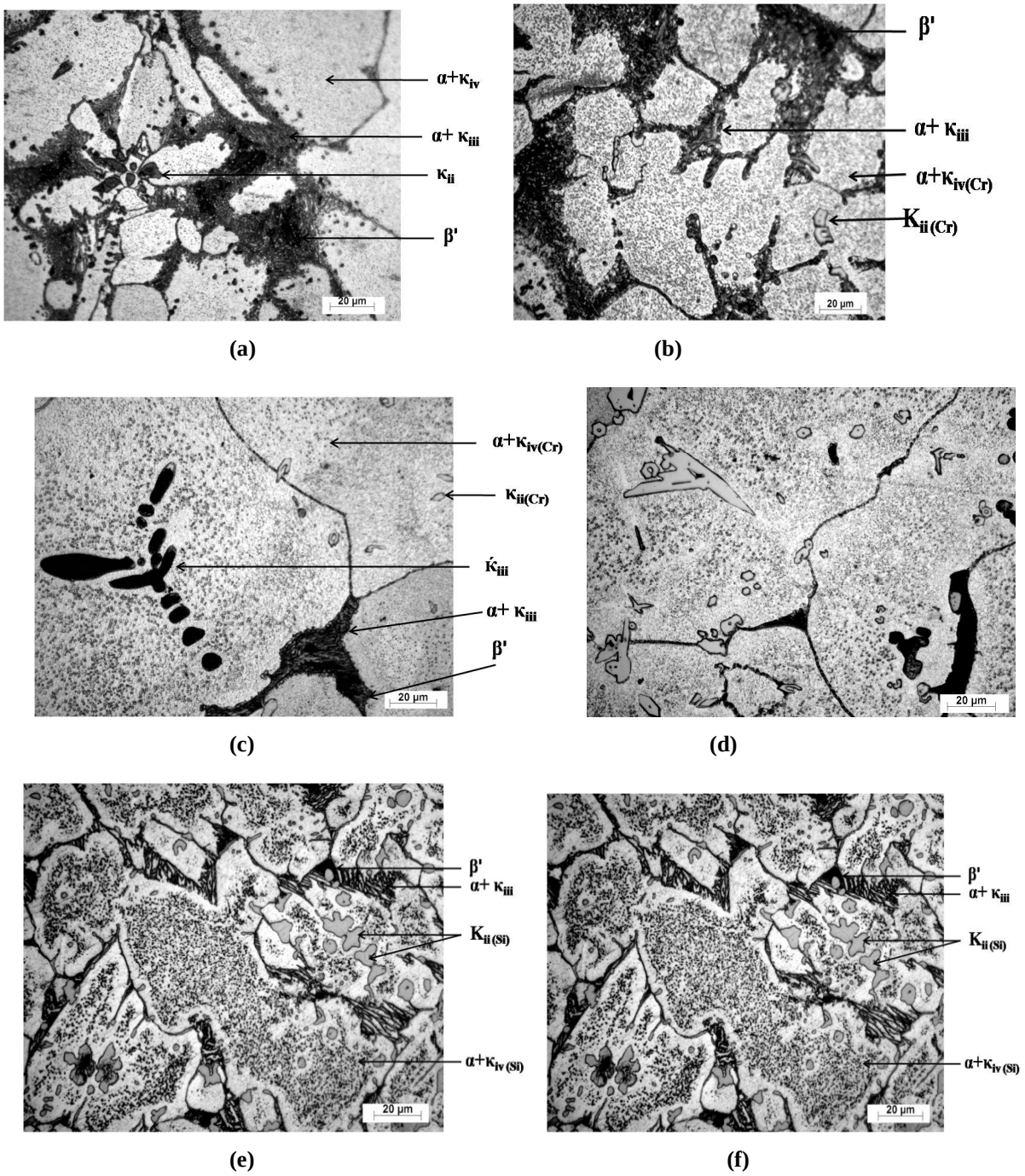

Figure 1: Optical Micrographs of the NAB Alloy with and Without Addition of Chromium and Silicon: (a) NAB; (b) NAB + 0.4Cr; (c) and (d) NAB + 0.8% Cr; (e) NAB + 0.5% Si; (f) NAB + 0.2% Cr + 0.5% Si

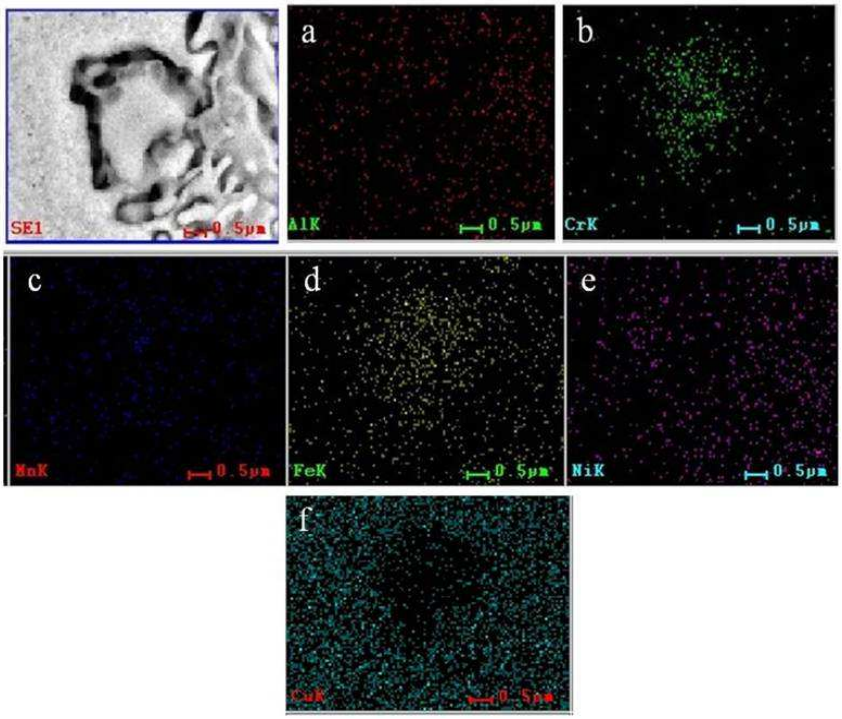

Figure 2: EDS Elemental Mapping of Al (A), Cr (B), Mn (C), Fe (D), Ni (E) and Cu (F) In $K_{ii\ (Cr)}$ Phase of NAB Alloy Treated with 0.4 Wt % Cr Showing that $K_{ii\ (Cr)}$ Phase was Exhausted Most of Iron and Chromium. This is Accompanied by a Decrease in the Concentration of Copper to a Low Limit

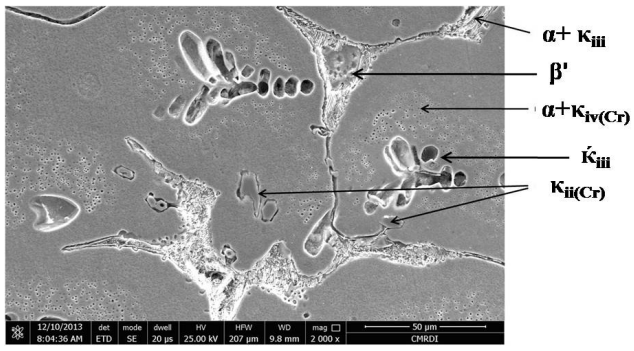

Figure 3: SEM Micrograph of NAB Alloys Treated with 0.8% Cr

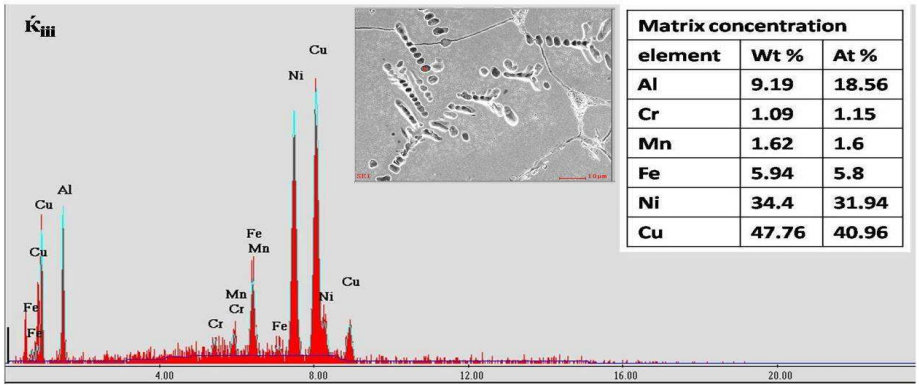

Matrix concentration		
element	Wt %	At %
Al	9.19	18.56
Cr	1.09	1.15
Mn	1.62	1.6
Fe	5.94	5.8
Ni	34.4	31.94
Cu	47.76	40.96

Figure 4: Energy Dispersion Spectrum (EDS) Showing Amounts and Distribution of Elements Al, Cr, Fe, Mn, Ni and Cu in $ḱ_{iii}$ Phases

SEM Microstructure

The scanning electron micrograph (SEM) in Figure 5 depicts the morphology of the κ phases in unmodified NAB alloy (a), alloy treated with 0.4 wt %Cr (b), and alloy treated with 0.5 wt% Si (c). It was evident from the micrographs that kappa phases have a dendritic morphology and precipitates at the grain boundary in unmodified alloy which led to alloy embrittlement Figure 5a.

It is confirmed in Figure 5b that the grain size of NAB + 0.4 Cr alloys is smaller than that of NAB alloys and κ phases become smaller than unmodified alloy. This inhibition of grain growth upon adding chromium is considered to be due to the formation of colonies of κ precipitates. The κ phases in the alloy treated with 0.5 wt% Si (Figure 5c) become globular in shape and well defined compared with unmodified alloy. Grain refinement was very significant with the addition of 0.5% Si to the NAB alloy. This was mainly attributed to the formation of fine κ precipitates and dispersed to be nucleation sites during solidification of the alloy.

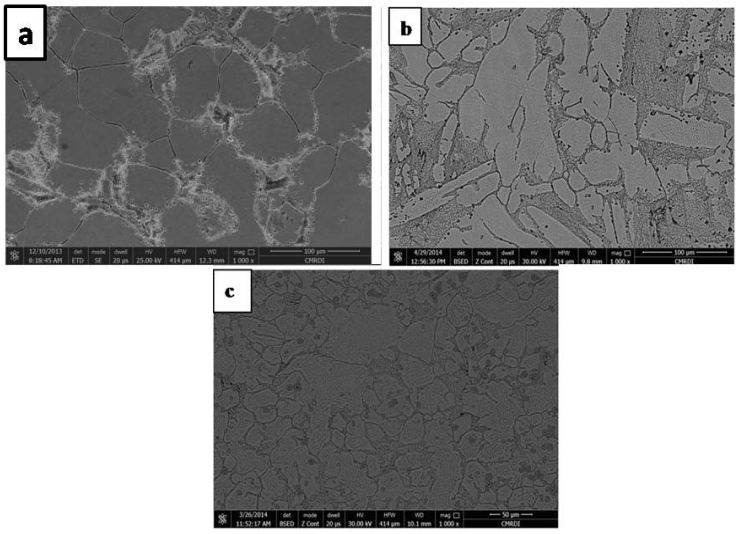

Figure 5: Scanning Electron Micrographs of NAB Alloy With and Without Addition of Chromium and Silicon: (a) NAB; (b) NAB + 0.4Cr; (c) NAB + 0.5% Si

MECHANICAL PROPERTIES

Tensile Properties

The data obtained for the ultimate tensile strength and percentage elongation of the basic alloy and modified alloys (Cr, Si, and (Cr+Si)) are presented in Table 2. Different strength and elongation combinations can be obtained through the addition of different modifier elements. The tensile properties of Cr and Si modified alloys are somewhat higher than that unmodified alloy. This is attributed to precipitation of fine/dendritic particles of κ phases. This finding reflects the fact mentioned earlier that the mechanical properties of the NAB casting alloys are largely dependent on the κ phase characteristics [19]. The ultimate tensile strength of the unmodified NAB alloy was 484 MPa, and elongation percent was 9.7%. This could be attributed to the presence of sparse distribution of κ precipitates in a predominant **α** matrix.

Addition of 0.4 Cr has increased the ultimate tensile strength (UTS) nominally to 522 MPa (8% improvement) compared to the unmodified alloy due to modification and refinement of intermetallic κ precipitates with small change in the percent elongation. When Cr addition increases to 0.8%, the modification effect of Cr decreases due to formation of κ precipitates rich in chromium and iron which consume most of chromium present in the alloy. This phase is hard and brittle

which may give way to permanent failure. Also, the complex compound rich in Cu and Ni ($ќ_{iii}$) that has formed in this alloy due to increasing amounts of Cu and Ni in the liquid precipitated in the separate groups in the matrix and decreases grain locking effect; so the UTS decreases to 403MPa and percent elongation decreases to 6%. Therefore, the addition of 0.5% Si to the NAB alloy has increased the UTS to 569 MPa and has a 16% improvement in the ductility. This effect is due to modification and refinement of κ phases resulting in decreasing alpha grain size. It has also been observed that the combined addition of Cr and Si increases somewhat the UTS to 512 MPa. This is accompanied by a considerable improvement of the elongation (39%) of the alloy as compared to the unmodified alloy.

Table 2: Tensile Properties of Tested Alloys

Alloy	Tensile (MPa)	Elongation (%)
NAB alloy	484	9.70
NAB+ 0.4% Cr	522	8.50
NAB + 0.8% Cr	403	7.50
NAB + 0.5% Si	569	11.3
NAB +0.2% Cr+ 0.5%Si	512	13.5

Hardness Results

Figure 6 and Table 3 give the average values of Vickers hardness of studied alloys and microhardness μHV of the phases α and $κ_{ii}$. The results indicated that the hardness of the NAB alloy is mainly affected by precipitation of hard κ phases. Addition of chromium and/or silicon to the NAB alloy increases the hardness of these precipitates resulting in improving the hardness of the alloy. Addition of 0.4 wt% Cr to the NAB alloy increases the macrohardness from 154 to 177. This is due to increase of amounts of hard $\boldsymbol{κ_{ii(Cr)}}$ precipitates. Chromium is aggregates to the **κ** phases and makes them hard complex compounds rich in Cr and Fe. For the alloy treated with 0.8% Cr, the hardness was decreased presumably due to withdrawal of more iron and chromium present in the matrix to form hard and brittle $\boldsymbol{κ_{ii\ (Cr)}}$ precipitates. As can be seen in Table 3, increased microhardness of $\boldsymbol{κ_{ii\ (Cr)}}$ precipitates in comparison with the initial NAB bronze is due to larger Cr dissolved in such phase. Increasing Cr content to 0.8% caused the μHV of $\boldsymbol{κ_{ii\ (Cr)}}$ precipitates increased from 226 to 420 and the μHV of phases **α** from 163 to 198**.** The significant increase in the μHV of $\boldsymbol{κ_{ii\ (Cr)}}$ phase due to large Cr and Fe quantities in this phase which make it very hard and brittle phase. The addition of 0.5 wt% silicon increases the macrohardness by 26% compared to unmodified alloy. It has a similar effect of hardening of precipitates and matrix. Combined addition of Cr and Si to NAB alloy caused a microhardness of $\boldsymbol{κ_{ii\ (CrSi)}}$ precipitates increase of 30%. This is due to larger concentration of Si dissolved in $\boldsymbol{κ_{ii\ (CrSi)}}$ precipitates.

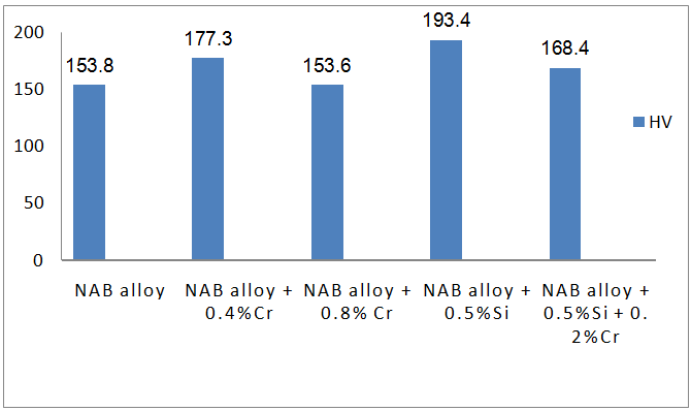

Figure 6: Effect of Cr, Si and Cr + Si Additions on the Macro Hardness HV of the NAB Alloy

Table 3: Effect Of Cr, Si and Cr + Si Additions on the Micro Hardness of A and K_{ii} Phases

Alloys	µHV α	µHV κ_{ii}
NAB Alloy	163 ± 2	226 ± 4
0.4 wt% Cr	215 ± 3	288 ± 2
0.8 wt% Cr	198 ± 12	420 ±6(*)
0.5 wt% Si	215 ± 3	275 ± 4
0.2 wt% Cr + 0.5 wt% Si	208 ± 2	293 ± 2

(*) This value represents the microhardness of an isolated κ_{ii} particle, whereas the other values were determined on a fine mixture of **(α+ κ_{ii})** phases.

WEAR RESULTS

The data collected from the wear test are presented in Figure 7. Obviously, marked improvement in the wear resistance was obtained due to modification of the basic NAB alloy with both chromium and silicon.

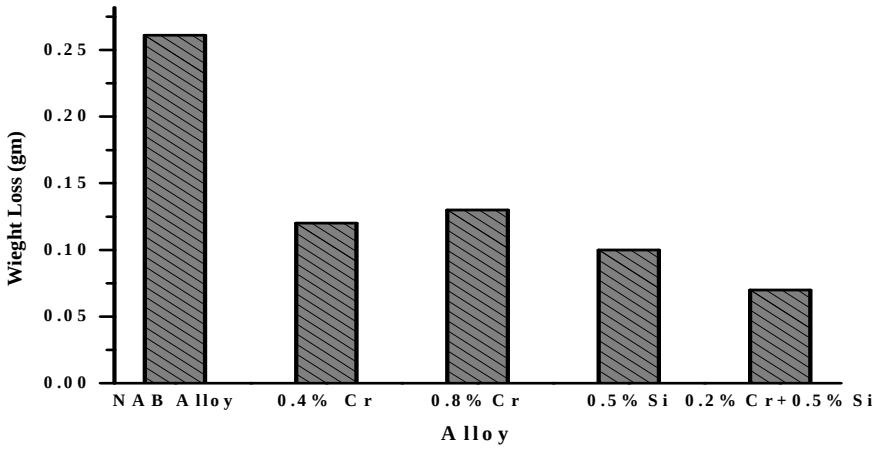

Figure 7: Effect of Cr, Si and Cr + Si Additions on the Weight Loss of NAB Alloy

The strengthening of the α-matrix is an important means of promoting the wear resistivity of NAB alloy. In addition to the modification of the hard $\kappa_{ii\ (Cr)}$ precipitates and decreasing α grain size, The best improvement in the wear resistance is obviously due to silicon addition particularly due to the combined addition of (Cr + Si). Again, this is due to dispersion hardening of the " harder " κ phase.

CONCLUSIONS

In the present investigation the following conclusions could be summarized as follows:

- The NAB alloy could be strengthened by precipitation of κ phases in α matrix after addition of Cr and Si; it was shown that the chromium and silicon could refine and modify the κ precipitates effectively. They make the κ phases crystallize as complex silicides rich in these elements and act as nuclei for heterogeneous nucleation.
- The addition of 0.4 wt% Cr to the NAB alloy improved the tensile strength (9%), hardness (15%) and wear resistance (60%) due to refinement of κ phases.
- On the other hand increasing the chromium contents to 0.8 wt% tends to lower the levels of these mechanical

properties. The EDS data confirm that κ_{ii} precipitates exhausted most of Cr and Fe present in the alloy which make them hard and brittle phases.

- Significant grain refinement was noticed after modification with 0.5 wt% Si. This may be attributed to the precipitation of complex silicides ($\kappa_{ii\ (Si)}$ **and** $\kappa_{iv\ (Si)}$ precipitates) that crystallized as spherical or fine dendrite crystals in the center of alloy grains, dispersed, and act as the nuclei of heterogeneous nucleation in the melt.
- The α-grain size can be controlled by addition of the modifying elements Cr and Si. The grain size of the NAB alloy decreased from 56 µm to 44 µm after the addition of 0.4% Cr. however, it increased when the amount of Cr reached to 0.8%. Silicon appears more powerful as grain refiner. After addition of 0.5 wt% Si to the NAB alloy, the grain size has decreased by 43%. With the combined addition of Cr and Si, the grain size decreased by 40% than when the modifier element was added separately.
- Optimum combination of tensile strength, ductility and wear resistance is attainable with (0.5 wt% of Si + 0.2 wt% of Cr) addition which is superior to the unmodified NAB alloy. The ultimate tensile strength was 511 MPa, the hardness was 182 HV, with a weight loss 0.08 gm. this is compared with 484 MPa, 153 HV and 0.3 gm of the basic NAB alloy.
- The significant effect of the combined additions of (Cr + Si) is the remarkable improvements of the wear resistance of the NAB alloy (70%). The hardening effect of this addition was associated with high level of ductility.

REFERENCES

1. Duma, J. A., 1975, “Heat Treatments For Optimizing Mechanical and Corrosion Resisting Properties of Nickel-Aluminum Bronzes”, Naval Engineers Journal, v. 87, pp. 45-64.
2. Anonymous, 1989, “Aluminum Bronze - Essential for Industry”, CDA, Publication No 86.
3. Radomila Konecná and Stanislava Fintová, 2012, “Copper and Copper Alloys: Casting, Casting, Classification and Characteristic Microstructures”, Copper Alloys - Early Applications and Current Performance – Enhancing Processes, March.
4. Brian K. Vazquez, 2003 “The Effects of Isothermal Deformation and Annealing on Nickel-Aluminum-Bronze Materials in Relation to the Friction Stir Process”, etc., MS Thesis, Naval Postgraduate School, Monterey, CA.
5. Yuanyuan LI, T. L. Ngai, 1996, “Grain Refinement and Microstructural Effects on Mechanical and Tribological Behaviors of Ti and B Modified Aluminum Bronze”, Journal of materials Science 31, pp. 5333-5338.
6. M. Mokhtari Shirazabad, A. Karimi, 2012, The Effect of Aging Treatment Parameters on Microstructure and Hardness of Aluminum Bronze Alloy”, ICMH.
7. Meigh, H., 2000, Cast and Wrought Aluminum Bronzes: Properties, Processes and Structure, Copper Development Association / IOM Communications, London.
8. F. Hasan, A. Jahanafrooz, G. W. Lorimer and N. Ridley, 1982, “The Morphology, Crystallography, and Chemistry of Phases in As-Cast Nickel-Aluminum Bronze,” Met. Trans A, v. 13a, pp.1337-1345.

9. Culpan, E. A. and Rose, G., 1978, “Miscrostructural Characterization of Cast Nickel Aluminum Bronze”, Journal of Materials Science, v. 13, pp. 1647-1657.
10. A. Jahanafrooz, E hasan, G. W. Lorimer, and N. Ridley, 1982, Microstructural Development in Complex Nickel-Aluminum Bronzes, Metallurgical Transactions A, v. 14A, pp. 1983-1951.
11. D. M. Lloyd, G. W. Lorimer, and N. Ridley, 1980, “Characterization of Phases in a Nickel-Aluminum Bronze”, Metals Technology, v. 7, pp. 114-119.
12. B. Pisarek, 2007, Influence Cr on crystallization and the phase's transformations of the bronze BA1044, Archives of Foundry Engineering, v. 7, Issue 3, pp. 129-136.
13. B. Pisarek, 2008 Abrasive wear of BA1055 bronze with additives of Si, Cr, Mo and/or W, Archives of Foundry Engineering, vol. 8, Issue 3, pp. 209–216.
14. B. Pisarek, 2008, The influence of wall thickness on the microstructure of bronze BA1055 with the additions of Si, Cr, Mo and/or W, Archives of Foundry Engineering, v. 8, Issue 4, pp. 185-192.
15. B. Pisarek, 2012, Effect of annealing time for quenching CuAl7Fe5Ni5W2Si2 bronze on the microstructure and mechanical properties, Archives of Foundry Engineering, V. 12, Issue2, pp. 187- 204.
16. B. Pisarek, 2010, Influence of the technology of melting and inoculation preliminary alloy AlBe5 on change of concentration of Al and microstructure of the bronze CuAl10Ni5Fe4, Archives of Foundry Engineering, v. 10, Issue 2, pp. 127-134.
17. B. Pisarek, 2011, Effect of additions of Cr, Mo, W and/or Si on the technological properties of aluminum-iron-nickel bronze, Archives of Foundry Engineering, v. 11, Issue 3, pp. 199- 208.
18. B. Pisarek, 2013, Model of Cu-Al-Fe-Ni Bronze Crystallization, Archives of Foundry Engineering, v. 13, Issue 3, pp.72-97.
19. J. Łabanowski, T. Olkowski, 2009, Effect of Chemical Composition and Microstructure on Mechanical Properties of BA1055 Bronze Sand Castings, Advances in Materials Science, V. 9, No. 1, pp. 19.